Catalysis Today 155 (2010) 271–278

Contents lists available at ScienceDirect

Catalysis Today

journal homepage: www.elsevier.com/locate/cattod

Nickel-catalyzed isomerization of 2-methyl-3-butenenitrile to 3-pentenenitrile: A kinetic study using *in situ* FTIR-ATR spectroscopy

Laura Bini [a], Erwin J.E. Houben [b], Evgeny A. Pidko [a], Christian Müller [a], Dieter Vogt [a,*]

[a] Department of Chemical Engineering and Chemistry, Schuit Institute of Catalysis, Eindhoven University of Technology, 5600 MB Eindhoven, The Netherlands
[b] DSM Resolve, Geleen, The Netherlands

ARTICLE INFO

Article history:
Available online 23 September 2009

Keywords:
Pentenenitriles
Isomerization
Operando technique
IR spectroscopy
IR probe

ABSTRACT

The isomerization of 2-methyl-3-butenenitrile (2M3BN) to 3-pentenenitrile (3PN) was followed using *operando* FTIR spectroscopy. The spectra were analyzed comprehensively to obtain kinetic profiles from the different band dynamics. Several spectral regions were transformed to their second derivative in order to improve the peak resolution. The dynamics in the spectra were calculated and normalized to the end conversion towards 3PN determined by GC. Similar kinetic profiles were obtained from the dynamics of different bands. Furthermore, calculations on the DFT level were performed for 2M3BN and *trans*- and *cis*-3PN in order to help identifying the corresponding bands in the spectra of the reaction mixture. An average conversion profile was calculated from different bands of the substrate and the product, applying a "*quasi*-multivariate analysis" technique to correlate different band dynamics. This approach was validated using advanced chemometrics. These profiles obtained by IR spectroscopic analysis for the formation of 3PN and the consumption of 2M3BN showed a zero order kinetic.

1. Introduction

The DuPont adiponitrile process is so far the only example of an industrial application of the Ni-catalyzed alkene hydrocyanation [1,2]. Adiponitrile (ADN) is produced from butadiene *via* hydrocyanation and isomerization reactions. The addition of HCN to butadiene leads to both the desired linear isomer 3-pentenenitrile (3PN) and the undesirable branched isomer 2-methyl-3-butenenitrile (2M3BN) in a variable ratio [1]. In the second step of the process, 2M3BN is isomerized to 3PN in the presence of the same nickel catalyst used for the hydrocyanation. This reaction proceeds through a C–CN bond breaking/forming reaction involving a [Ni(II)allyl(cyanide)] complex (Scheme 1) [3,4].

Both hydrocyanation and isomerization reaction are closely related. While the Ni(II) intermediate is formed in the hydrocyanation reaction by HCN addition to the metal complex a Ni(II) species is also formed by the oxidative addition of 2M3BN to a Ni(0) precursor in one of the first steps of the catalytic isomerization reaction [5–7]. Moreover, the reductive elimination of nitriles, that is believed to be the rate-determining step [8], takes place as the last step of the cycle in both hydrocyanation and isomerization reactions. The isomerization can thus be considered as a model reaction for *in situ* studies of the mechanism and the kinetics of the rate-limiting step of the hydrocyanation reaction. In combination with $Ni(cod)_2$, all classes of bidentate phosphorus ligands, such as phosphines, phosphinites, phosphonites, and phosphites catalyze the isomerization [9–11]. The influence of the ligand parameters on the catalyst activity for this reaction still remains unknown.

The first challenge is to find a suitable technique for the *in situ* experiments. So far, the investigations have been limited to a few papers reporting on the characterization of the isomerization reaction intermediates by NMR spectroscopy, using phosphine ligands [12–15]. However, *in situ* NMR studies on this reaction are difficult. In fact, the tetrahedral coordination geometry that can occur with the Ni(II) intermediates, causes the presence of paramagnetic species [16].

Tolman [17] and Druliner [18] have already reported on the characterization of Ni complexes by IR spectroscopy. In their work the interaction of zero-valent nickel phosphite complexes with various independent components of the catalytic system, such as HCN and different olefins, has been investigated, aiming for a better understanding of the mechanism.

In our studies the isomerization of 2M3BN was performed and for the first time the reaction was followed by *operando* FTIR-ATR spectroscopy [19,20–22]. In fact, using IR spectroscopy, the detection is not negatively influenced by the presence of paramagnetic species. A kinetic profile was obtained by analyzing the dynamics of the bands in the IR spectra. DFT calculations were used to confirm the band assignments.

* Corresponding author at: Department of Chemical Engineering and Chemistry, Schuit Institute of Catalysis, Eindhoven University of Technology, P.O. Box 513, 5600 MB Eindhoven, The Netherlands. Tel.: +31 40 2472483; fax: +31 40 2455054.
E-mail address: D.Vogt@tue.nl (D. Vogt).

0920-5861/$ – see front matter © 2009 Elsevier B.V. All rights reserved.
doi:10.1016/j.cattod.2009.08.017

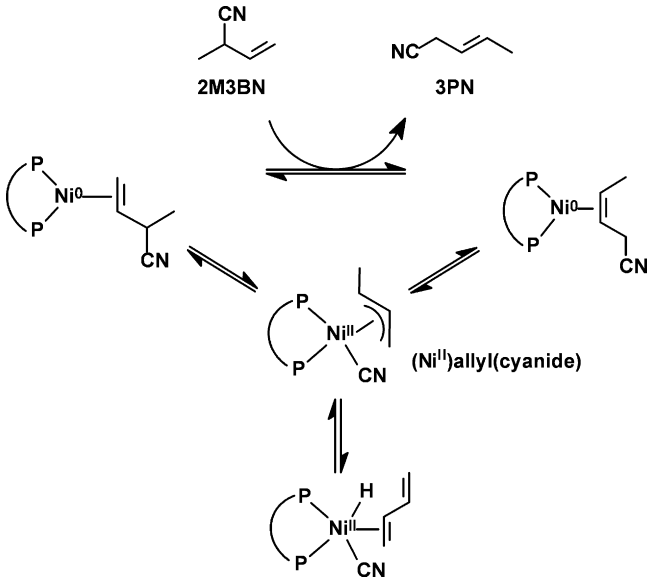

Scheme 1. Isomerization of 2M3BN.

2. Experimental

2.1. General considerations

Chemicals were purchased from Aldrich, Acros or Merck and used as received. 1,4-Dioxane was distilled over CaH_2 prior to use. All preparations were carried out under an argon atmosphere using standard Schlenk techniques. 1,8-(Bis-diphenylphosphino)triptycene [23] and $Ni(cod)_2$ [24] were synthesized according to literature procedures. IR spectra were recorded on a Nicolet Avatar 360 FTIR instrument connected to a Remspec IR Fiber-Optic Immersion Probe. The spectra were recorded and elaborated using an Omnic E.S.P. 5.2a program. The light transmission efficiency of this setup is less than 20% and consequently the sensitivity was relatively low. High concentrated samples and long collection times (up to 7 min) were required, implying that fast reactions cannot be monitored with this specific setup.

2.2. General procedure for the isomerization experiments

A solution of ligand (23.0 mg, 0.036 mmol) in 2 mL of dioxane was added to $Ni(cod)_2$ (10.0 mg, 0.036 mmol) in a Schlenk tube and stirred for 5 min. 2M3BN (400 μL, 200 equiv.) was added with an Eppendorf pipette, followed by 100 μL of *n*-decane as internal standard. A diamond ATR deep immersion probe connected to a FTIR instrument with a flexible light guide was immersed in the reaction mixture. The Schlenk tube was placed in an oil bath and heated to 60 °C. IR spectra were recorded every 10 min. A sample for GC-analysis was taken after 4 h. The selectivity is defined as 3PN/(Σ nitriles).

2.3. IR spectra

Number scans	700
Resolution	4 cm^{-1}
Data spacing	1.929 cm^{-1}
Gain	4
Velocity	1.8988 cm/s
Spectral range	4000–900 cm^{-1}

2.4. IR data treatment

The FTIR spectra were transformed into the absorbance mode. Further data treatment was performed using the PerkinElmer software Spectrum v5.0.1. All spectra were normalized using the C–H def. vibrational band originating from the dioxane solvent. The peak maximum at 1365 cm^{-1} was set at ordinate 1.0 with a one sided base point at 1340 cm^{-1}. The second derivative spectra were calculated applying 13 points. In both, the absorbance spectra as well as the second derivative spectra, the peak heights are linear with the concentration as given by the Lambert–Beer law. The peak heights were determined at 3055, 2248, 1478 and 1434 cm^{-1} using fixed base points in the nearest maxima at both sides using the t = 170 min spectrum.

2.5. Multivariate analyses

The multivariate calculations were performed in MATLAB R2006B (The Mathworks, Inc.) using the PLS toolbox version 4.2 (Eigenvector Research, Inc.). Multi Curve Resolution (MCR) was applied to the set of spectra in the interval 1500–1400 cm^{-1} with the constraints that the output must contain only non-negative pure spectra and non-negative concentrations. The calculation of the first two components captured >98% of the variation in the spectra. The resulting profile was normalized to the end conversion of 87% determined by GC.

2.6. Computational details

Quantum chemical calculations were carried out in the framework of density functional theory using the Gaussian 03 program [25]. The hybrid B3LYP functional was used in a combination with the 6-311+G(d,p) basis set in all computations. No symmetry restrictions were imposed during the geometry optimization. The nature of the calculated structures was evaluated from the analytically computed harmonic normal modes. All of the optimized structures showed no imaginary frequencies and thus were assumed to correspond to the local minima.

3. Results and discussion

3.1. IR spectra: interpretation and kinetic profiles

The isomerization was performed in dioxane at 60 °C for 4 h using a triptycene-based diphosphine ligand [23] (Fig. 1) and $Ni(cod)_2$ as the metal precursor. IR spectra were recorded every 10 min using a diamond ATR probe connected to an FTIR instrument with a flexible light guide or deep immersion probe.

In the isomerization reaction, the branched unsaturated nitrile 2M3BN is converted *via* C–CN bond cleavage to the linear nitrile alkene, 3PN (Scheme 1). Therefore, the nitrile bands are most characteristic for this reaction. The vibration involved is the stretching of the triple bond, which occurs at 2260–2240 cm^{-1} in aliphatic nitriles [26] (Fig. 2). Since this region of the spectrum is relatively free of other signals, even weak bands can be distinctive and reliable.

The overlaying of the spectra showed no further dynamics of the bands after 170 min. Consequently, the reaction was complete

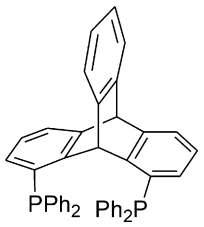

Fig. 1. Triptycene-based diphosphine ligand.

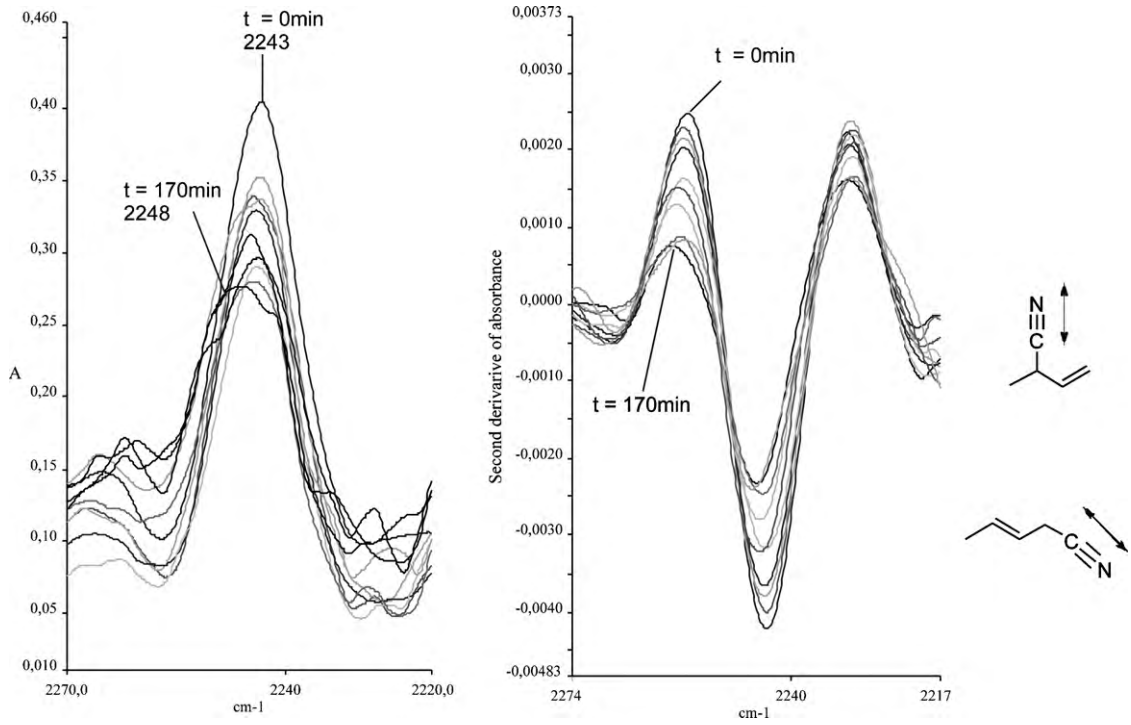

Fig. 2. Absorbance spectra (left) and 2nd derivative spectra (right) of the –CN region.

after the first 3 h and only these spectra will be discussed. The band at 2243 cm^{-1} is assigned to the nitrile stretch vibration of 2M3BN. This band showed a decrease in intensity and peak broadening, while the formation of 3PN was confirmed by the appearance of a nitrile absorption at 2248 cm^{-1}. The two bands are not well resolved (Fig. 2).

Therefore, second derivative spectroscopy was applied for the interpretation of these spectra. This technique consists in calculating the second derivative of the absorption spectrum with respect to the frequency [27]. According to Beer's law, the second derivative of the absorbance spectrum is linear in concentration. In the second derivative spectra improved peak resolution is observed, which can be associated to the formation of 3PN and the consumption of 2M3BN (Fig. 2).

A total conversion of 87% in this experiment was determined after 4 h by GC-analysis. The dynamics in the spectra were calculated by integration methods and normalized to the final conversion. Nitrile isomers, other than 2M3BN and 3PN, were detected only in traces. A kinetic profile for the formation of 3PN was obtained [28], as shown in the Fig. 9. It should be mentioned here that the use of the deep immersion probe does not allow a fast temperature change. In other words, the probe needs a slow equilibration to have the best detection conditions. Therefore, the temperature was slowly increased from room temperature to 60 °C during 40 min. During this period the reaction does not lead to significant 3PN formation.

The initial IR spectrum recorded at the start of the reaction, when only 2M3BN is present in the reaction mixture, was taken as

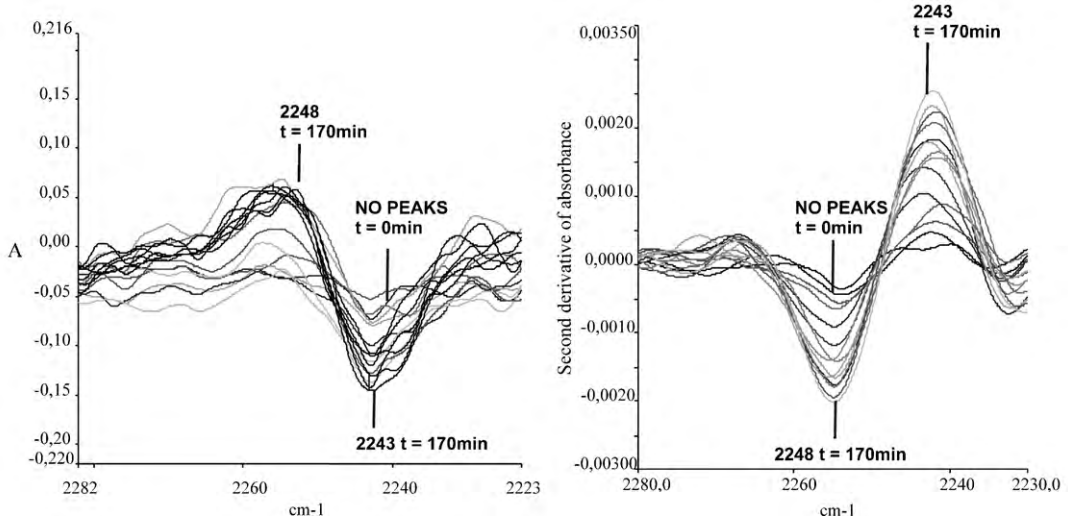

Fig. 3. Absorbance spectra (left) and 2nd derivative spectra (right) of the –CN region after subtraction of the spectrum recorded at the initial time (only 2M3BN).

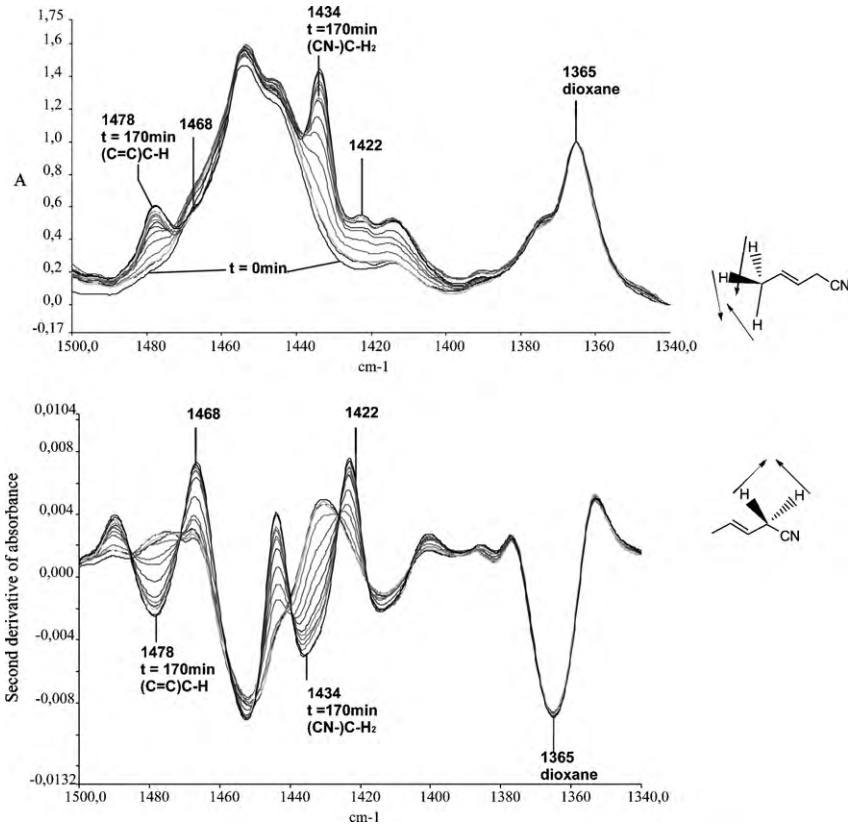

Fig. 4. Absorbance spectra (upper) and 2nd derivative spectra (lower) for the C–H band region.

background spectrum and subtracted from the spectra recorded during the isomerization experiment (Fig. 3). Consequently, the initial difference spectrum does not show any bands in the nitrile region. The following difference spectra show the formation of a new band at 2248 cm^{-1} related to 3PN and a negative band at 2243 cm^{-1} related to the consumption of 2M3BN. Using the second derivative, a smoothing function is applied. The peaks get better resolved and the kinetics can be calculated more accurately, due to less noise variation on the selected base points.

Stretching and deformation vibrations characterize methyl and methylene groups. In aliphatic compounds, the asymmetric out-of-phase $-CH_3$ deformation occurs near 1465 cm^{-1}, although the methyl wave numbers show some sensitivity to the electronegativity of the attached atoms [29]. The $-CH_2-$ deformation bands [30], which are located near 1463 cm^{-1} in alkenes, is lowered to about 1440 cm^{-1} when the $-CH_2-$ group is next to a double or a triple bond. A carbonyl, nitrile, or nitro group each lowers the frequency of the adjacent $-CH_2-$ group to approximately 1425 cm^{-1} and increases its intensity [31]. The –CH– deformation [32] appears as a weak band at 1350–1315 cm^{-1}.

The C–H deformation band region was analyzed in the dynamic IR spectra of the isomerization reaction. A band originating from

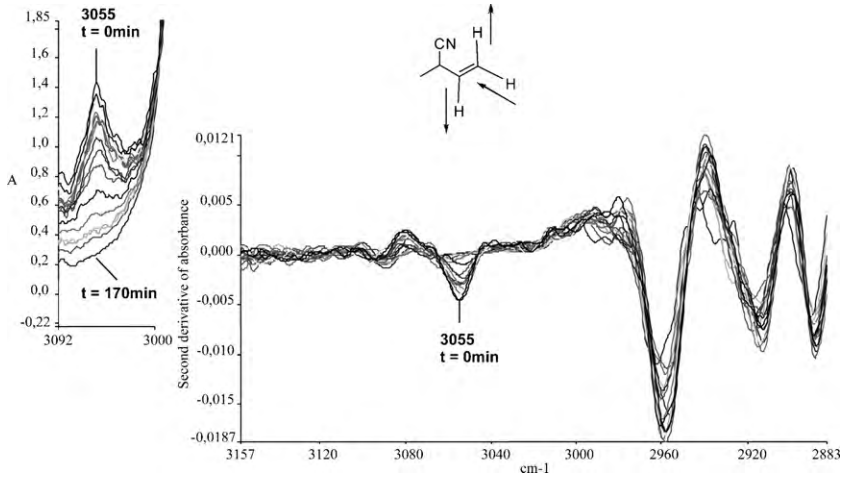

Fig. 5. Absorbance spectra (left) and 2nd derivative spectra (right) for the (C=)C–H stretching band.

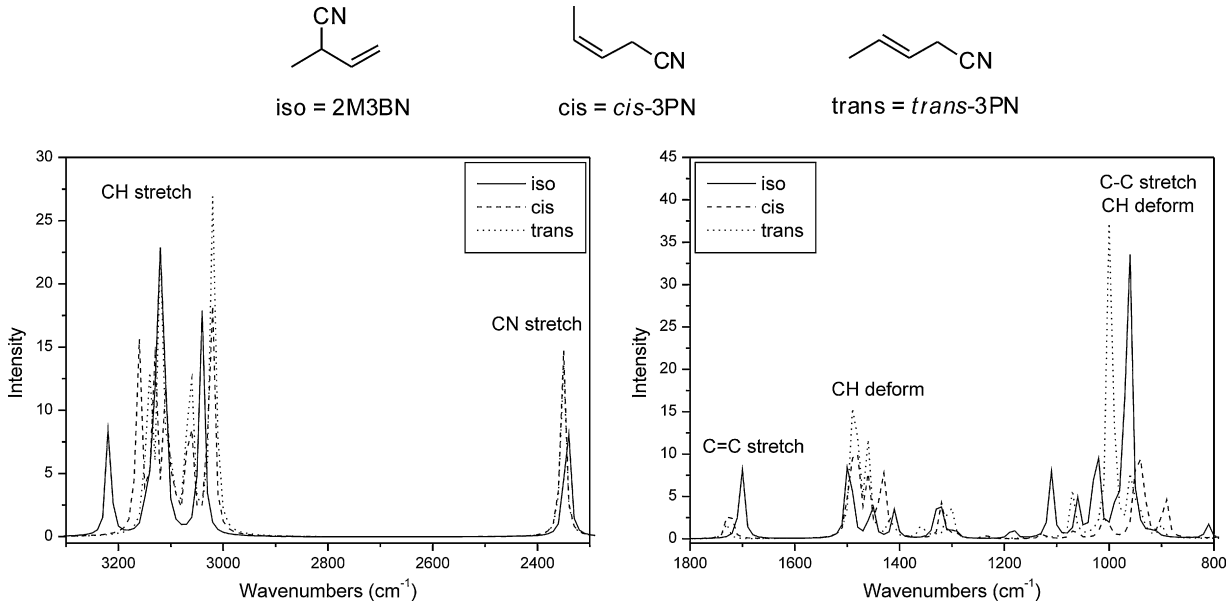

Fig. 6. Overlaid spectra of 2M3BN, *cis*- and *trans*-3PN. The spectra are obtained from DFT calculations. Hybrid B3LYP functional was used in a combination with the 6-311+G(d,p) basis set.

the solvent was present at 1365 cm^{-1} (dioxane C–H twisting band) [33] and used to normalize the IR spectra. Other bands clearly showed dynamic transformations, although there is extensive overlapping of the peaks. The peak intensities of the bands at 1478 and 1434 cm^{-1} evolve during the reaction. The two bands are assigned to the methyl and the methylene group C–H deformation of 3PN, respectively (Fig. 4).

The second derivative allowed again having a clearer pattern for the peak intensity, especially for the band at 1478 cm^{-1}. The kinetic profiles obtained for these dynamics were similar to the one for the nitrile group (Fig. 9).

Olefinic =CH– stretching occurs at 3130–2980 cm^{-1}. In particular, the out-of-phase $=CH_2$ stretch vibrations of vinyl compounds (monosubstituted ethylenes) give rise to a band in the region 3100–3070 cm^{-1} in hydrocarbons [34]. This band is well separated from other =CH– stretching bands below 3000 cm^{-1}.

2M3BN contains a vinyl group. Therefore, also the (C=)C–H stretch band region was taken into consideration. The peak intensity at 3055 cm^{-1} decreases during the reaction (Fig. 5). The 2nd derivative of the spectra allows an improved calculation of the kinetic profile (Fig. 9). The calculation was made considering the 2M3BN consumption during the formation of 3PN: 3PN(%) = 100 − 2M3BN(%). The obtained graph shows a kinetic curve similar to the three previous ones, calculated from the nitrile, methyl and methylene 3PN bands.

3.2. DFT calculations and peak assignment

The simplest description of a vibration is a harmonic oscillator [35]. Applying this concept, it is possible to use computational methods to gain insights into the vibrational motion of molecules. There are a number of computational methods available with varying degrees of accuracy [36]. Frequencies computed with a quantum harmonic oscillator approximation tend to be 10% higher than the experimental value, due to the approximation itself and the lack of electron correlation. Most studies are done using *ab*

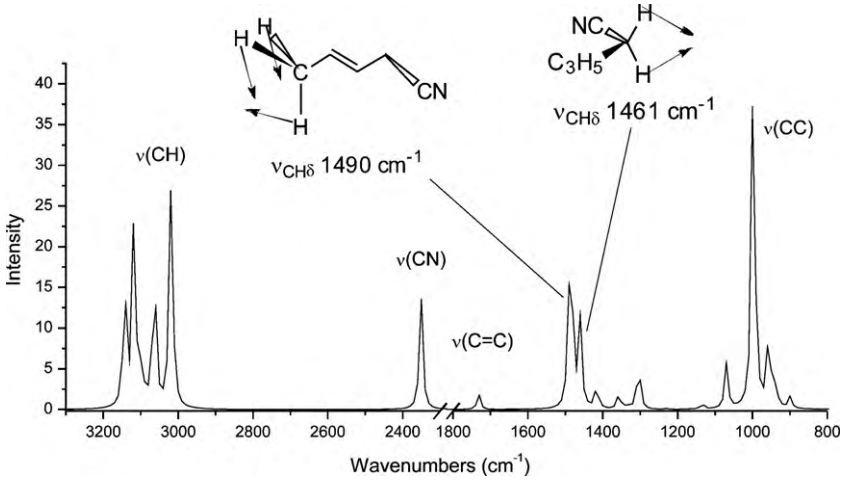

Fig. 7. DFT calculation of the 3PN IR spectrum, assignment of the deformation bands for the methyl and methylene groups. Hybrid B3LYP functional was used in a combination with the 6-311+G(d,p) basis set.

initio methods. The overall systematic error is less with DFT calculations [37].

Another related issue is the computation of the intensities of the peaks in the spectrum. Peak intensities depend on the probability that a particular wavelength photon will be absorbed and are obtained by computing the transition dipole moments as relative peak intensities, since the calculation does not include the density of the substance.

The DFT calculations were used to confirm the peak assignment in the spectra obtained from the reaction mixture and to study the formation of *trans*- and *cis*-3PN independently. Calculations for 2M3BN, as well as for *trans*- and *cis*-3PN were performed and the spectra were superimposed as shown in Fig. 6. The frequency values showed a shift to higher wave numbers compared to the experimental results, but the general trend is confirmed. The nitrile bands for the products (*trans*- and *cis*-3PN) have higher wave numbers than the band for the substrate (2M3BN). The C–H deformation bands are in a very narrow spectral region and not completely resolved. The same overlapping is observed in the C–H stretching region, except for the vinyl (C=)C–H band. Unfortunately, isolated peaks of *cis*- or *trans*-3PN were identified only in the finger print region (900–1000 cm^{-1}). The IR light guide used during the experiment, limited the spectral range in the low wave number region giving very low signal to noise ratio. Consequently, the formation of these two products could not be investigated separately.

Figs. 7 and 8 show the spectra of 3PN and 2M3BN and, in particular, the vibrations identified in the experimental spectra. The methyl and methylene groups were detected at 1478 and 1434 cm^{-1}, respectively and the calculations showed that these vibrations occur at 1490 and 1461 cm^{-1}. For the vinyl C–H stretching band, a shift was observed from 3055 cm^{-1} in the experimental to 3218 cm^{-1} in the calculated spectrum. The shift increases at higher wave numbers, because the error in the calculations becomes bigger for larger motions of the harmonic oscillator. However, the peak positions maintain the same trend. It can be concluded that DFT calculations confirm the peak identification that we proposed for the experimental spectra.

3.3. "Quasi-multivariate" analysis

The profiles calculated from the different IR bands presented similar dynamics, but show also a considerable error range (Fig. 9). This error is due to the low peak to noise ratio in the IR spectra recorded during the isomerization experiment. There are two main reasons for the low peak to noise ratio. The low light transmission through the ATR probe has a negative effect on the noise level of the whole spectrum. On the other hand, low signal to noise ratio was detected mainly in the high frequency range (>1500 cm^{-1}). The path length through the reaction mixture and subsequently the absorbance (peak intensity) are inversely related to the frequency. In other words, the depth of penetration (d_p) is directly related to the wave length (λ). Furthermore, a systematic error was introduced *via* the integration method that involves the arbitrary choice of the base line points and the peak maxima.

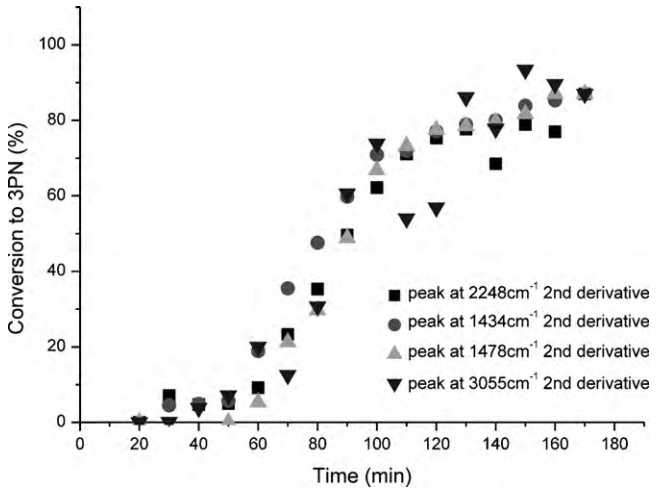

Fig. 9. Kinetic profiles obtained from the –CN stretching, the $-CH_3$ and $-CH_2-$ deformation and the $=CH_2$ stretching bands, for the formation of 3PN and the consumption of 2M3BN.

Due to such complexity of the samples, more sophisticated methods of data analysis are now being used, such as the multivariate analysis technique [38,39]. As the name indicates, multivariate analysis comprises a set of techniques dedicated to the analysis of data sets with more than one variable. In the IR spectra each frequency can be regarded as one variable. Several of these techniques were developed in the last 20 years, because they require the computational capabilities of modern computers.

A "*quasi*-multivariate" (QMV) analysis was applied to the spectra recorded for the isomerization of 2M3BN. Each band

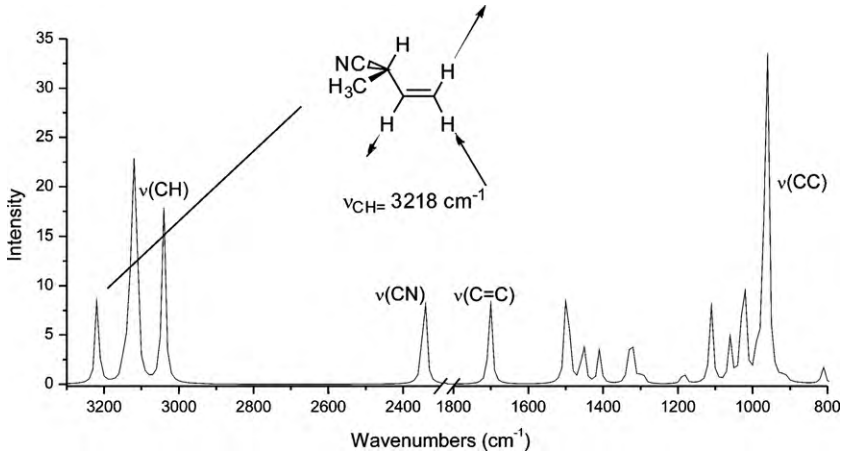

Fig. 8. DFT calculation of the 2M3BN IR spectrum, assignment of the stretching band for the vinyl group. Hybrid B3LYP functional was used in a combination with the 6-311+G(d,p) basis set.

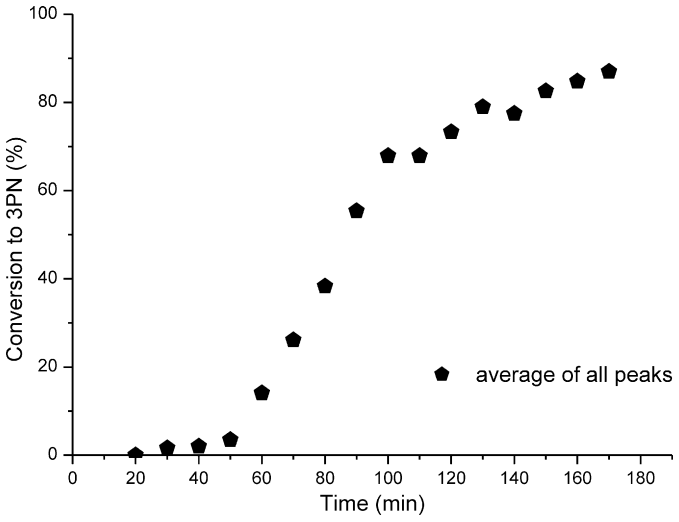

Fig. 10. Kinetic profile obtained as average of the four kinetic profiles of different IR bands.

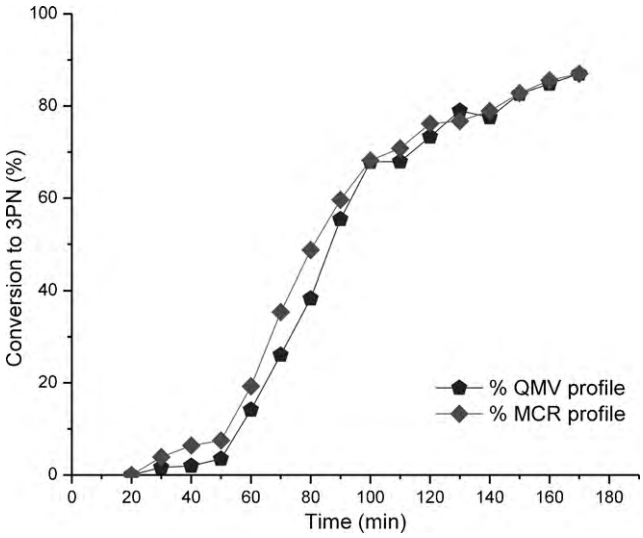

Fig. 11. Superimposed QMV and MCR kinetic profiles.

dynamic in the spectra was considered as a different variable and an average kinetic profile was calculated (Fig. 10). The profile was obtained by averaging the conversions for each recording time. The aim was to minimize the error in the average profile compared to the single band dynamic one. This method is an easy approach to make use of the correlation between different band dynamics, in order to increase the accuracy of the kinetic profile. In fact, the formation of 3PN and the consumption of 2M3BN are taken into consideration simultaneously, being directly correlated in the reaction and, consequently, showing the same kinetics.

3.4. Multivariate analysis

The IR data were further analyzed by chemometrics, which is the application of mathematical or statistical methods to chemical data. The method used was the multivariate curve resolution (MCR) [39,40]. The –CH– deformation region of the IR spectra was chosen for the multivariate analysis (see Supplementary Material). In fact, this region presents a lower peak to noise ratio, leading to a lower residue matrix and consequently more accurate chemometric calculation. The kinetic profile calculated from the multivariate analysis is depicted below (Fig. 11). The profile obtained via a *quasi*-multivariate analysis is superimposed in Fig. 11. The two profiles show a reasonably good agreement, which validates the results obtained with the first more accessible method for analyzing the data (QMV).

Due to the limitations of the setup used, a series of experiments carried out at different concentrations and temperatures could not be performed, in order to analyze the kinetics of the reaction. However, the profile for the isomerization of 2M3BN at 60 °C and in the presence of the [NiTripty(PPh_2)$_2$] catalyst suggests zero order for the 2M3BN consumption and the 3PN formation [10]. The first 3% of conversion are neglected, since the temperature of the reaction mixture needed to be equilibrated slowly. The last 20% of conversion are also not taken into account because of catalyst deactivation. The profiles obtained with the QMV and the MCR methods both show a good linear fitting, while a logarithmic fitting, which would indicate a first order, does not apply (Fig. 12).

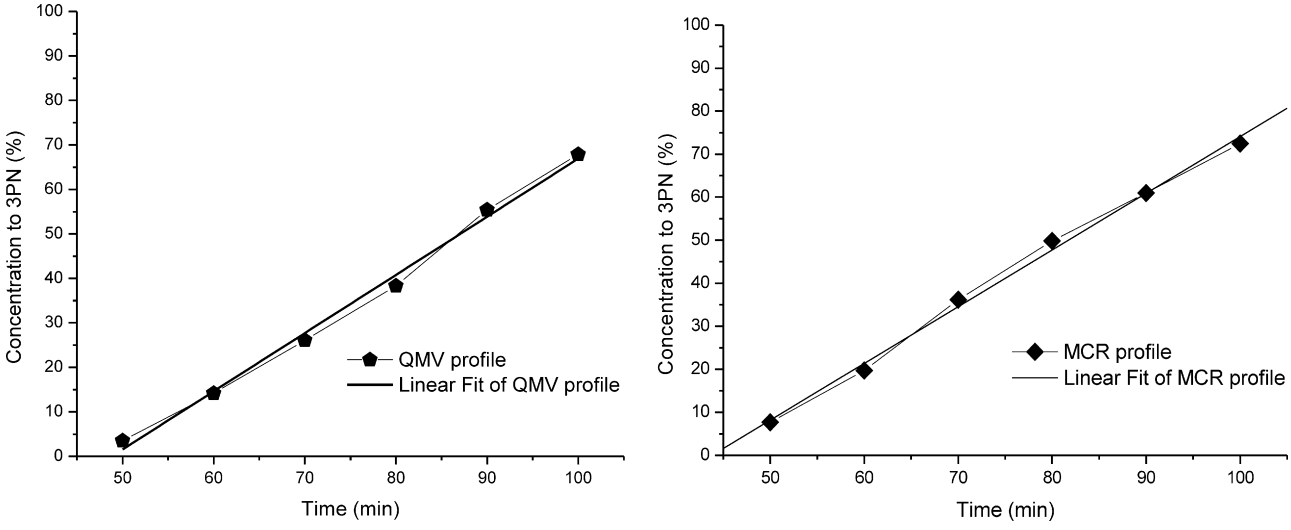

Fig. 12. Linear fitting for the QMV and MCR kinetic profile.

4. Conclusions

The isomerization of 2M3BN was performed in dioxane at 60 °C for 4 h using a triptycene-based diphosphine ligand in combination with $Ni(cod)_2$. A final conversion of 87% was determined by GC-analysis. IR spectra were recorded every 10 min using an ATR probe connected with a flexible light guide to a FTIR instrument.

Different regions in the spectra were analyzed. The peak in the –CN stretch region at 2243 cm^{-1} gradually decreased and a second peak at 2248 cm^{-1} arose, while the 2M3BN is converted into 3PN. Also the CH deformation and the (C=)CH stretch regions showed transformations in time. Several spectral regions have been transformed to their second derivative. The dynamics in the spectra were calculated and normalized to the final conversion determined by GC. Similar kinetic profiles were obtained from the dynamics of different bands. Furthermore, DFT calculations have been performed to obtain calculated IR spectra of 2M3BN, *trans*- and *cis*-3PN, in order to assign the corresponding bands in the spectra of the mixture. An average kinetic profile was obtained from the dynamics of four different peaks in the spectra applying a "*quasi*-multivariate" analysis (QMV), taking into consideration the correlated formation of 3PN and consumption of 2M3BN.

A chemometric analysis of the CH deformation region generated a profile similar to the one obtained *via* QMV. The latter method was, therefore, validated as a more accessible approach to make use of the correlation between different band dynamics of the significant spectral regions.

For the first time IR spectroscopy was applied to determine the kinetics of the 2M3BN isomerization reaction. Improvements in the FTIR setup would allow in the future the application of such spectroscopic method also to the study of the hydrocyanation reaction.

Acknowledgements

This work has been financially supported by the National Research School Combination on Catalysis (NRSCC) and by Evonik Oxeno. C.M. thanks The Netherlands Organization for Scientific Research (NWO-CW) for financial support. The authors gratefully acknowledge Peter Tummers and Ton Staring for technical assistance.

Appendix A. Supplementary data

Supplementary data associated with this article can be found, in the online version, at doi:10.1016/j.cattod.2009.08.017.

References

[1] K. Huthmacher, S. Krill, in: B. Cornils, W.A. Hermann (Eds.), 2nd ed., Applied Homogeneous Catalysis with Organometallic Compounds, vol. 1, Wiley-VCH, Weinheim, 2002, p. 465.
[2] C.A. Tolman, Chem. Rev. 77 (1977) 313.
[3] A. Chaumonnot, F. Lamy, S. Sabo-Etienne, B. Donnadieu, B. Chaudret, J.C. Barthelat, J.C. Galland, Organometallics 23 (2004) 3363.
[4] K. Nakamoto, Infrared and Raman Spectra of Inorganic and Coordination Compounds, 3rd ed., Wiley, 1978.
[5] J.I. van der Vlugt, A.C. Hewat, S. Neto, R. Sablong, A.M. Mills, M. Lutz, A.L. Spek, C. Müller, D. Vogt, Adv. Synth. Catal. 346 (2004) 993.
[6] A. Acosta-Ramirez, M. Muñoz-Hernandez, W.D. Jones, J.J. Garcia, J. Organomet. Chem. 691 (2006) 3895.
[7] A. Acosta-Ramirez, M. Muñoz-Hernandez, W.D. Jones, J.J. Garcia, Organometallics 26 (2007) 5766.
[8] W. Goertz, W. Keim, D. Vogt, U. Englert, M.D.K. Boele, L.A. van de Veen, P.C.J. Kamer, P.W.N.M. van Leeuwen, J. Chem. Soc. Dalton Trans. (1998) 2981.
[9] T. Foo, J.M. Garner, Tam, WO 99/06357 (1999), Chem. Abstr., 130 (1999) 169815.
[10] M. Bartsch, R. Baumann, D.P. Kunsmann-Keitel, G. Haderlein, T. Jungkamp, M. Altmayer, W. Siegel, F. Molnar, DE 10150286 (2003), Chem. Abstr., 138 (2005) 304408.
[11] C.P. Lenges, WO 03/076394 (2003), Chem. Abstr., 139 (2006) 262467.
[12] N.M. Brunkan, D.M. Brestensky, W.D. Jones, J. Am. Chem. Soc. 126 (2004) 3627.
[13] J. Wilting, C. Müller, A.C. Hewat, D.D. Ellis, D.M. Tooke, A.L. Spek, D. Vogt, Organometallics 24 (2005) 13.
[14] A. Acosta-Ramirez, A. Flores-Gaspar, M. Muñoz-Hernandez, A. Arevalo, W.D. Jones, J.J. Garcia, Organometallics 26 (2007) 1712.
[15] B.D. Swartz, N.M. Reinartz, W.W. Brennessel, J.J. Garcia, W.D. Jones, J. Am. Chem. Soc. 130 (2008) 8548.
[16] G. Maki, J. Chem. Phys. 15 (1958) 5.
[17] C.A. Tolman, W.C. Seidel, J.D. Druliner, P.J. Domaille, Organometallics 3 (1984) 33.
[18] J.D. Druliner, Organometallics 3 (1984) 205.
[19] N.J. Harrick, Internal Reflection Spectroscopy, Wiley, New York, 1967.
[20] P.R. Griffiths, J.A. de Haseth, Fourier Transform Infrared Spectroscopy, Wiley, New York, 1986.
[21] B.M. Weckhuysen, Chem. Commun. (2002) 97.
[22] M.O. Guerrero-Perez, M.A. Banarez, Chem. Commun. (2002) 1292.
[23] L. Bini, C. Müller, J. Wilting, L. von Chrzanowski, A.L. Spek, D. Vogt, J. Am. Chem. Soc. 128 (2006) 11374.
[24] R.A. Schunn, Inorg. Synth. 15 (1974) 5.
[25] M.J. Frisch, G.W. Trucks, H.B. Schlegel, G.E. Scuseria, M.A. Robb, J.R. Cheeseman, J.A. Montgomery Jr., T. Vreven, K.N. Kudin, J.C. Burant, J.M. Millam, S.S. Iyengar, J. Tomasi, V. Barone, B. Mennucci, M. Cossi, G. Scalmani, N. Rega, G.A. Petersson, H. Nakatsuji, M. Hada, M. Ehara, K. Toyota, R. Fukuda, J. Hasegawa, M. Ishida, T. Nakajima, Y. Honda, O. Kitao, H. Nakai, M. Klene, X. Li, J.E. Knox, H.P. Hratchian, J.B. Cross, V. Bakken, C. Adamo, J. Jaramillo, R. Gomperts, R.E. Stratmann, O. Yazyev, A.J. Austin, R. Cammi, C. Pomelli, J.W. Ochterski, P.Y. Ayala, K. Morokuma, G.A. Voth, P. Salvador, J.J. Dannenberg, V.G. Zakrzewski, S. Dapprich, A.D. Daniels, M.C. Strain, O. Farkas, D.K. Malick, A.D. Rabuck, K. Raghavachari, J.B. Foresman, J.V. Ortiz, Q. Cui, A.G. Baboul, S. Clifford, J. Cioslowski, B.B. Stefanov, G. Liu, A. Liashenko, P. Piskorz, I. Komaromi, R.L. Martin, D.J. Fox, T. Keith, M.A. Al-Laham, C.Y. Peng, A. Nanayakkara, M. Challacombe, P.M.W. Gill, B. Johnson, W. Chen, M.W. Wong, C. Gonzalez, J.A. Pople, Gaussian 03, Revision B 05, Gaussian, Inc., Pittsburgh, PA, 2003.
[26] E. Kitson, N.E. Griffith, Anal. Chem. 24 (1952) 334.
[27] M.R. Whitbeck, Appl. Spectrosc. 35 (1981) 93.
[28] H. Susi, D.M. Byler, Biochem. Biophys. Res. Commun. 115 (1983) 391.
[29] N. Sheppard, Trans. Faraday Soc. 51 (1955) 1465.
[30] N. Sheppard, D.M. Simpson, Quart. Rev. Chem. Soc. 7 (1953) 19.
[31] L.J. Bellamy, R.L. Williams, J. Chem. Soc. Lond. (1956) 2753.
[32] J.J. Fox, A.E. Martin, Proc. Roy. Soc. Ser. A 167 (1938) 257.
[33] F.E. Malherbe, H.J. Berustein, J. Am. Chem. Soc. 17 (1952) 4408.
[34] H.L. McMurry, Thornton, Anal. Chem. 24 (1952) 318.
[35] E.B. Wilson Jr., J.C. Decius, P.C. Cross, Molecular Vibrations: The Theory of Infrared and Raman Vibrational Spectra, Dover, New York, 1980.
[36] D.C. Young, Computational Chemistry: A Practical Guide for Applying Techniques to Real-World Problems, Wiley, New York, 2001.
[37] R.J. Meier, Vib. Spectrosc. 43 (2007) 26.
[38] H. Martens, T. Naes, Multivariate Calibration, Wiley, New York, 1989.
[39] P.H.G. Tummers, E.J.E. Houben, J.F.G.A. Jansen, D. Wienke, Vib. Spectrosc. 43 (2007) 116.
[40] K.L.A. Chan, S.G. Kazarin, Appl. Spectrosc. 61 (2007) 48.